Available online at www.sciencedirect.com
ScienceDirect
Polymer 47 (2006) 7070–7077
polymer
www.elsevier.com/locate/polymer

Structure and mechanical properties of PGA crystals and fibres

H. Montes de Oca[1], I.M. Ward*

IRC in Polymer Science and Technology, School of Physics and Astronomy, University of Leeds, Leeds LS2 9JT, UK

Received 9 June 2006; received in revised form 19 July 2006; accepted 22 July 2006
Available online 17 August 2006

Abstract

The elastic constants of poly(glycolic acid) (PGA) crystals are reported on the basis of a commercial software package and the published crystal structure of the polymer. Due to the planar zigzag conformation of the molecular chains, very high elastic anisotropy is found with a tensile chain modulus of 294 GPa and a longitudinal shear modulus for a fibre of 6 GPa. A combination of small and wide angle X-ray scattering and differential scanning calorimetry are used to characterise the structure of highly oriented PGA fibres. The combination of long period data, crystal size and crystallinity measurements suggests a structure similar to the Prevorsek model, with alternating crystalline and amorphous regions along the fibre axis, and layers of amorphous material in parallel. A parallel–series Takayanagi model, using the theoretically calculated chain modulus, is shown to give good agreement with the experimental data in a wide temperature range.

Keywords: Mechanical properties; Structure; PGA

1. Introduction

Poly(glycolic acid) (PGA) is a semi-crystalline polyester with good mechanical and degradative properties. PGA is biocompatible and in the body degrades via a hydrolysis reaction in which glycolic acid (GA) is the degradation product [1]. GA is decomposed in the carbohydrate cycle within the body, making PGA and some of its co-polymers very attractive for use in biomedical applications as sutures and as bone fixation devices in the form of pins, rods, plates and screws. Other applications of these materials include drug delivery carriers and scaffolds for cell culture [2,3].

Previous structural studies on PGA by X-ray diffraction indicate that two planar zigzag molecules pass through an orthorhombic unit cell with dimensions $a = 5.22$ Å, $b = 6.19$ Å and $c = 7.02$ Å (fibre axis) and space group $Pcmn - D_{2h}^{16}$ [4]. The chain axis has a twofold screw symmetry along the *c*-axis and the first chain lies on the *ac* plane at *b*/4, whereas the second chain, which is the mirror image of the first chain rotated 180° about *c*/2 lies on the *ac* plane at 3*b*/4 [4]. Recently, structural studies of highly oriented PGA by proton NMR spectroscopy [5] suggested that the ester group may not necessarily acquire a *trans*-planar conformation. However, the deviations from this, if any, are small and difficult to elucidate by X-ray diffraction, but appeared during more refined structural calculations of proton–proton dipole interactions within the crystal. Similar conclusions have also been suggested during structural studies of other linear polyesters (poly(ε-caprolactone)) by electron diffractometry [6].

Several studies have focused on the strength retention during degradation [7–11], but limited information is available in the literature in regard to the mechanical behaviour of PGA fibres [12] and to our knowledge the mechanical behaviour of PGA crystals is reported in this paper for the first time. The structure–processing–property relationships of PGA have been studied by Fu et al. [9,10] but this research group did not study in greater detail the mechanical behaviour of PGA fibres and crystals. As we shall see later, we obtain similar results to those published by Fu et al. in regard to the structure developed during processing, which together with the elastic properties of amorphous and crystalline

* Corresponding author. Tel.: +44 113 343 3808; fax: +44 113 343 3846.
E-mail address: i.m.ward@leeds.ac.uk (I.M. Ward).
[1] Current address: Smith & Nephew Research Centre, York Science Park, Heslington, York YO10 5DF, England.

0032-3861/$ - see front matter © 2006 Elsevier Ltd. All rights reserved.
doi:10.1016/j.polymer.2006.07.045

PGA form the basis to understand the elastic behaviour of highly oriented PGA fibres.

Our aim in this article is to study the structure and mechanical behaviour of oriented PGA crystals and fibres, presenting a consistent model for the tensile mechanical behaviour on the basis of structural data, theoretical calculations and experimental crystal strain measurements.

2. Experimental methods

"Amorphous" PGA fibres approximately 0.5 mm in diameter were kindly supplied by Smith & Nephew Research Centre, York, England. The fibres were drawn at 110 °C up to a draw ratio of 6 using the zone-drawing technique [13]. Small and wide angle X-ray scattering (SAXS and WAXS, respectively) measurements were undertaken using pinhole collimated X-rays in separate experiments using laboratory scale X-ray generators ($\lambda = 1.54$ Å) and the station 16.1 of the Synchrotron Radiation Source ($\lambda = 1.41$ Å) at the CLRC Daresbury Laboratory. SAXS measurements were obtained using a two-dimensional RAPID area detector calibrated with wet rat-tail collagen and with a sample to detector distance of 4.5 m. Ion chambers were placed before and after the sample in order to normalise the recorded intensities. Crystal strain measurements were obtained with the aid of an INEL curved multiwire linear detector calibrated with high-density polyethylene (HDPE) and silicon powder. A single fibre of circular cross-section was clamped horizontally in a house built extensometer with which the sample is strained by adding a series of loads, measuring the crystal strain after several minutes. Preliminary creep tests in a wide temperature range established conditions for full recovery of the fibre after removal of the load, ensuring that the crystal strain measurements were obtained in the elastic region of the fibre. Crystal strain measurements at low temperature were obtained by using a cryosystem that allows the control of the temperature of the fibre. WAXS photographs were obtained using a CCD camera calibrated with HDPE and silicon powder. Differential scanning calorimetry (DSC) measurements were carried out using a Perkin Elmer DSC7 calibrated with indium. Variations in the concavity and slope of the baseline curve were corrected until a satisfactory flat baseline was obtained. The storage modulus (E') was obtained over a wide temperature range using a Rheometrics Solids Analyser RSA II operated at 1 Hz with a dynamic strain of 0.05% and a heating rate of 4 °C/min.

3. Results and discussions

3.1. Theoretical elastic constants of PGA crystals

Theoretical elastic constants of PGA were obtained with the Materials Studio Software (Accelrys Inc.). The software requires the Cartesian coordinates of the atoms within the unit cell and for PGA these were obtained from the studies carried out by Chatani et al. [4], which together with the space group of the lattice can help one to generate the position of all the atoms within the unit cell. Once the crystal was built, the unit cell was optimised by finding the initial potential energy of the system arising from van der Waals and Coulomb interactions, allowing the unit cell angles to vary. Negligible changes in the unit cell parameters were found during the cell optimisation. The elastic constants (at 0 K) were obtained by minimising the potential energy of the strained crystal. The COMPASS force field was used and periodic boundary conditions were imposed. Non-bonded interactions were subject to an atom-based cut off of 9.5 Å for van der Waals interactions, while Ewald summation was used for Coulomb interactions. To confirm our procedures, a full set of elastic constants for the polyethylene (PE) crystal were determined and compared with the results of previous theoretical studies. Very good agreement was obtained with the results reported by Tashiro et al. [14] and Lacks and Rutledge [15].

Fig. 1 shows a schematic representation of the crystal structure of PGA proposed by Chatani et al. [4] and Table 1 shows the full set of elastic properties obtained with the Accelrys software. Before proceeding, it is important to clarify the nomenclature: the relationship between the suffixes *ij* and the axes of the crystal unit cell is as follows. The suffixes 1, 2 and 3 correspond to the directions defined by *a*, *b* and *c* axes of the unit cell, respectively, whereas 4, 5 and 6 relate to shear in the *bc*, *ac* and *ab* planes of the unit cell, respectively. In this paper we follow the convention used by Ward [16] in which a strain is caused in the *i* direction due to the stress applied along the *j* axis.

PGA shows a very high degree of elastic anisotropy, similar to that obtained for PE, with the highest stiffness constant C_{33} along the *c*-axis (the chain axis) where deformation involves bond bending and bond stretching. The lateral stiffness constants C_{11} and C_{22} are one order of magnitude lower because these primarily involve the weaker van der Waals intermolecular dispersion forces. The longitudinal shear stiffness constants C_{44} and C_{55} are low compared to C_{11}, C_{22} and C_{33}, reflecting the comparatively easy shear of the chains past each other. The low value of C_{66} is less expected and can be associated with the planarity of the chains. The Poisson's ratios ν_{31} and ν_{21} indicate that a force applied along the 1 axis (or the *a* axis) causes a larger contraction of the *b* axis than along the chain direction. The small positive value of S_{23} is not physically plausible and we conclude that it must represent an error in the calculations. This suggests that ν_{23} and ν_{32} must be close to zero, i.e., deformation of the *b* and *c* axes is negligible when a force is applied along *c* and *b* axes, respectively. Nevertheless the *a* axis shows some degree of compressibility, as indicated by ν_{12} and ν_{13}.

3.2. Elastic constants of a cylindrically symmetric aggregate of PGA crystals

Oriented fibres possess transverse isotropy due to their fibre symmetry and therefore it is useful to study the fibre properties on the basis of the elastic properties of an aggregate of crystals with cylindrical symmetry. The elastic behaviour of solids can be considered to lie between the limits of homogeneous stress (Reuss average) and uniform strain (Voigt average). To obtain

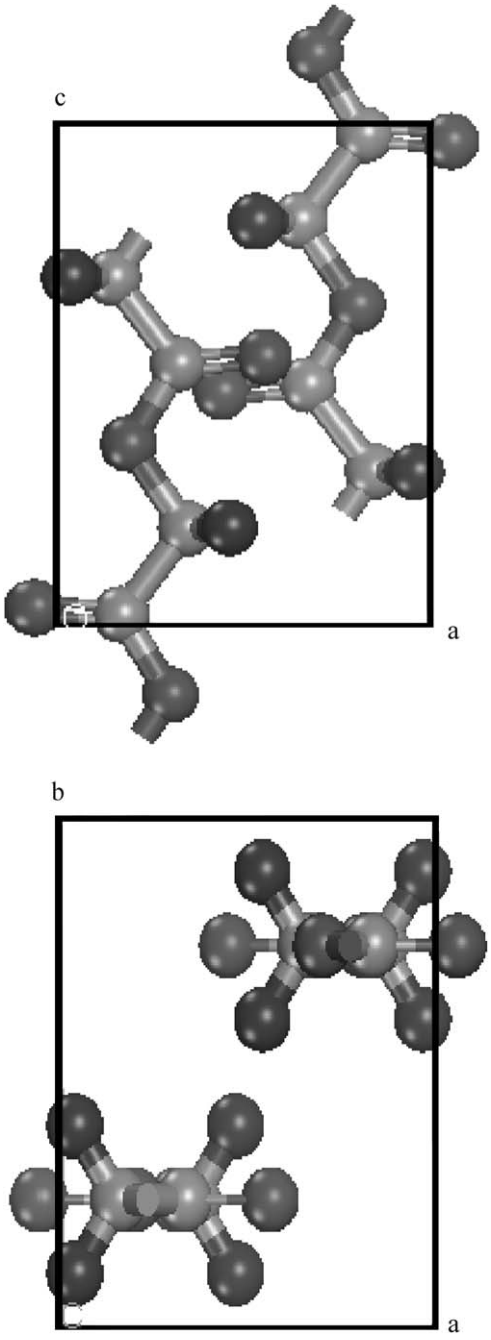

Fig. 1. Crystal structure of PGA.

the elastic properties of an aggregate of crystals with cylindrical symmetry on the basis of the elastic properties of the crystals for these two bounds it is required to carry out tensor averaging procedures for the compliances and stiffnesses about the chain axis of the crystals. These two averaging procedures provide lower and upper bounds for the elastic constants of the fibre, respectively. For a more comprehensive treatment of these procedures the reader is referred to Refs. [16,17].

Table 2 shows the elastic constants of a cylindrically symmetric aggregate of PGA [18] for the two bounds. The calculated fibre constants are very similar to those for other highly

Table 1
Elastic properties of PGA crystal

$$C_{ij} = \begin{pmatrix} 29.33 & 7.42 & 11.22 & 0 & 0 & 0 \\ 7.42 & 25.64 & 1.82 & 0 & 0 & 0 \\ 11.22 & 1.82 & 296.0 & 0 & 0 & 0 \\ 0 & 0 & 0 & 5.08 & 0 & 0 \\ 0 & 0 & 0 & 0 & 7.59 & 0 \\ 0 & 0 & 0 & 0 & 0 & 1.30 \end{pmatrix} \text{(GPa)}$$

$$S_{ij} = \begin{pmatrix} 3.73 & -1.07 & -0.13 & 0 & 0 & 0 \\ -1.07 & 4.2 & 0.02 & 0 & 0 & 0 \\ -0.13 & 0.02 & 0.34 & 0 & 0 & 0 \\ 0 & 0 & 0 & 19.68 & 0 & 0 \\ 0 & 0 & 0 & 0 & 13.18 & 0 \\ 0 & 0 & 0 & 0 & 0 & 76.98 \end{pmatrix} \left(\text{GPa}^{-1}\right) \times 100$$

$\nu_{ij}(-)$
$\nu_{12} = 0.25$
$\nu_{21} = 0.28$
$\nu_{13} = 0.38$
$\nu_{31} = 0.03$
$\nu_{23} = -0.06$
$\nu_{32} = -0.004$

Table 2
Elastic constants of a cylindrically symmetric aggregate of PGA crystals

Elastic property	Calculated bounds	
	Uniform strain (Voigt bound)	Homogeneous stress (Reuss bound)
E_1 (GPa)	16.9	8.1
E_3 (GPa)	294	294
G (GPa)	6.34	6.09
ν_{12}	0.51	0.77
ν_{13}	0.19	0.16
ν_{31}	0.01	0.01

oriented fibres such as polyethylene and polyethylene terephthalate [16] with $E_3 \gg E_1 > G$. The Poisson's ratios also reflect the high stiffness in the fibre axis direction, with a very low value of ν_{31}, and a comparatively high value of ν_{12}, showing that deformation is very much easier in the 1 and 2 directions than in the very stiff 3 direction.

3.3. Structure of highly oriented PGA

Fig. 2 shows a WAXS photograph (in symmetrical transmission [19]) of highly oriented PGA fibres where the (110), (020) and (002) reflections can be clearly identified. The WAXS photographs were analysed using the Image-Pro Plus software and from the azimuthal scan of the (002) reflection the orientation average $\sin^2\rho = 0.006$ was obtained (ρ is the angle between the fibre axis and the c-axis of the unit cell), indicative of a highly oriented crystalline structure, in agreement with orientation measurements by ^{1}H NMR spectroscopy [5,18].

The intensity patterns along the meridian and equator are shown in Figs. 3 and 4, from which the crystallite size (L_{hkl}) can be obtained with the aid of the Scherrer equation given by [20]:

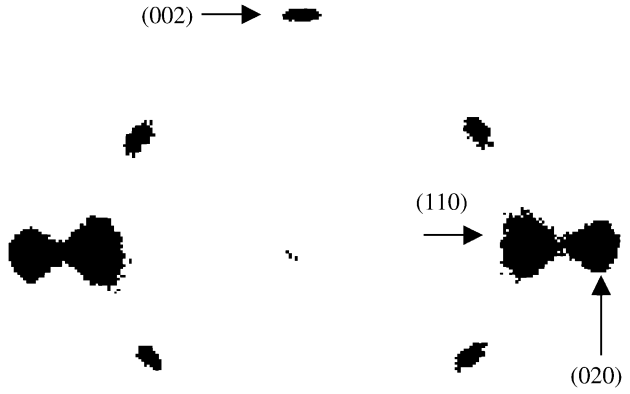

Fig. 2. WAXS pattern of highly drawn PGA fibres. Fibre axis along the meridian.

$$L_{hkl} = \frac{K\lambda}{\beta_0 \cos\theta} \tag{1}$$

where $K = 0.89$, θ the Bragg's angle, λ the wavelength of the X-rays and β_0 the corrected angular width at half maximum [20].

β_0 has to be corrected for instrumental broadening and for this purpose silicon powder was used as a calibration standard, assuming that the intrinsic broadening of the powder is negligible compared with the instrumental broadening. Since the peaks shown in Figs. 3 and 4 and the peak obtained from the calibration standard can be well described by Lorentzian functions, the corrected width at half maximum is given by [19]:

$$\beta_0 = \beta_{\text{obs}} - \beta_{\text{inst}} \tag{2}$$

where β_{obs} is the observed angular width at half maximum and β_{inst} is the instrumental broadening obtained from the calibration standard.

Fig. 5 shows the SAXS pattern of highly oriented PGA fibres where the maximum intensity observed in the meridian suggests the presence of alternating amorphous and crystalline

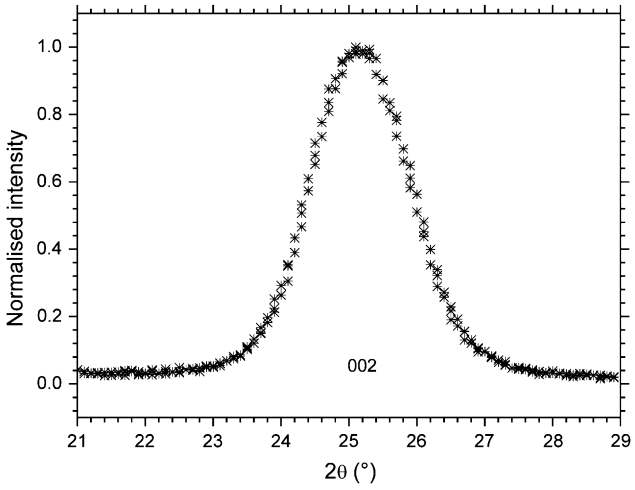

Fig. 3. WAXS intensity profile of the (002) reflection of highly drawn PGA fibres ($\lambda = 1.54$ Å).

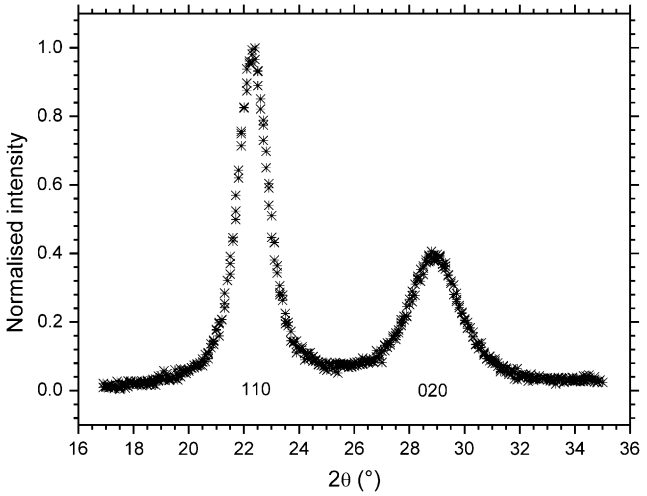

Fig. 4. WAXS intensity profile of the (110) and (020) reflections of highly drawn PGA fibres ($\lambda = 1.54$ Å).

regions along the fibre axis. Fig. 6 shows the SAXS intensity profile where the intensity pattern was projected onto the q scale obtained from the calibration with wet rat-tail collagen ($q = 4\pi \sin\theta/\lambda$). From the q value of the peak in Fig. 6 a long period of 80 Å was obtained using the equation:

$$L = \frac{2\pi}{q} \tag{3}$$

From the DSC measurements the heat of fusion (ΔH_{f}) of oriented PGA was obtained. Assuming a heat of fusion of an infinite crystal ($\Delta H_{\text{f}}^{\text{o}} = 139$ J/g [21]), a crystallinity of 50% was obtained with the aid of the following equation:

$$X = \frac{\Delta H_{\text{f}}}{\Delta H_{\text{f}}^{\text{o}}} \tag{4}$$

Table 3 shows the structural parameters of highly oriented PGA obtained from the WAXS, SAXS and DSC analyses described above. From the values of L_{110}, L_{020} and L_{002} it is reasonable to idealise the crystallites as rectangular prisms whose base is $L_{020}\sqrt{L_{110}^2 - L_{020}^2}$ and height is L_{002}. It is important to

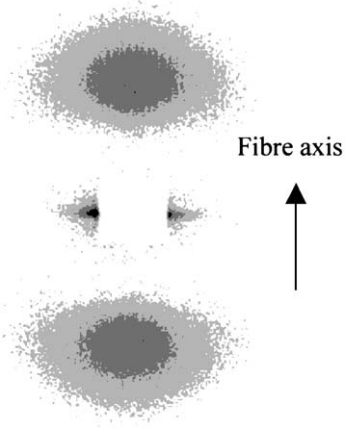

Fig. 5. SAXS pattern of highly drawn PGA fibres.

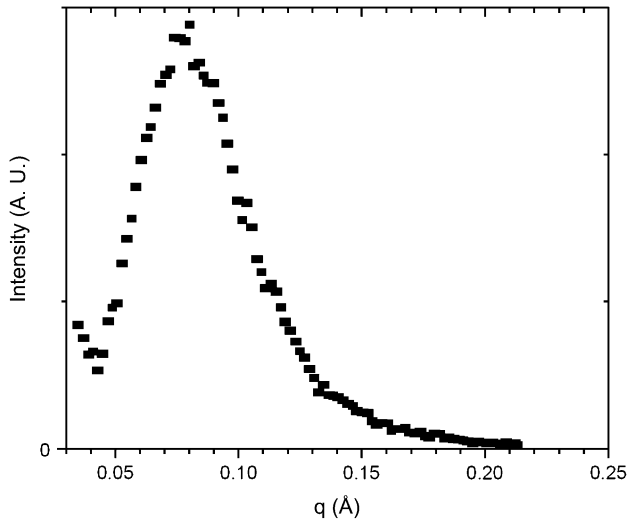

Fig. 6. SAXS intensity pattern of highly oriented PGA fibres.

note that the ratio $L_{002}/L = 0.86$ is considerably greater than the value of 0.5 for the crystallinity measured by ^{1}H NMR, DSC and density [18], suggesting that a more adequate description of the morphology of highly oriented PGA must include some amorphous material in parallel with the crystals. This three-dimensional model can be further simplified to two dimensions by assuming that the crystallites are embedded within fibrils that extend along the fibre axis, giving rise to the morphology shown in Fig. 7, originally proposed by Prevorsek for poly(ethylene terephthalate) fibres [22]. In Fig. 7, b_a (see Table 3) denotes the dimensions of a layer of amorphous material connected in parallel with blocks of alternating amorphous and crystalline regions, where $L_a = L - L_{002}$ is the size of the amorphous regions connected in series with the crystals. It is interesting to point out that according to the structural data in Table 3, the amorphous material connected in series with the crystallites represents only about 16% of the total amorphous material in the structure, mainly because $L_{002}/L = 0.86$. From the model in Fig. 7 the fraction of crystals can be written as:

$$X = \frac{L_{020}L_{002}}{L(b_a + L_{020})} \tag{5}$$

where b_a represents the thickness of the amorphous region in parallel with the crystallites, L is the long period and L_{020} and L_{002} are the crystallite dimensions in the direction parallel to the normal of the (020) and (002) crystallographic planes,

Table 3
Structural parameters of highly oriented PGA fibres

X (%)	L (Å)	L_{110} (Å)	L_{020} (Å)	L_{002} (Å)	L_a (Å)	b_a (Å)
50	80	43	26	69	11	19

b_a represents the width of amorphous material in parallel with the crystallites, L is the long period, L_{110}, L_{020} and L_{002} are the crystallite dimensions in the direction parallel to the normal of the (110), (020) and (002) crystallographic planes, respectively, and L_a is the thickness of the amorphous layer connected in series with the crystallites (see Fig. 7).

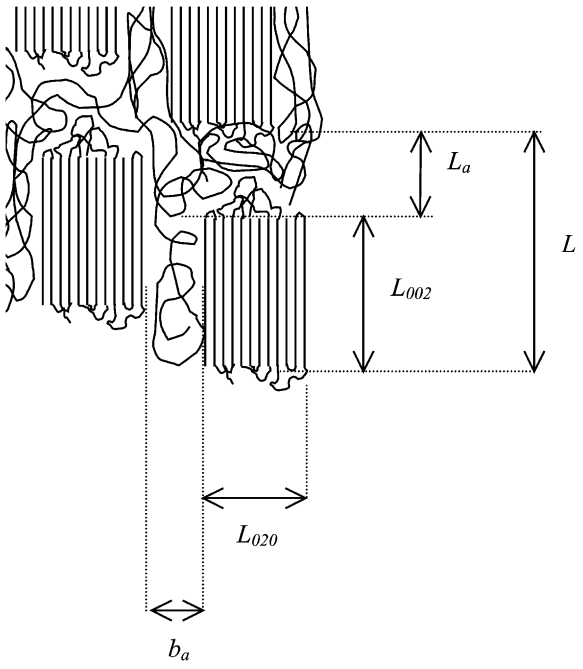

Fig. 7. Structure of highly oriented PGA fibres. b_a represents the width of amorphous material in parallel with the crystallites, L is the long period, L_{020} and L_{002} are the crystallite dimensions in the direction parallel to the normal of the (020) and (002) crystallographic planes, respectively, and L_a is the thickness of the amorphous layer connected in series with the crystallites.

respectively. From Eq. (5) b_a can be easily obtained and is shown in the last column of Table 3.

3.4. Mechanical behaviour of PGA fibres

In the previous section we have proposed a model for the structure of highly oriented PGA fibres and now we shall focus our attention on the mechanical behaviour of this structure along the fibre direction. First it is convenient to simplify the structure in Fig. 7 into its elementary constituents in order to analyse its mechanical behaviour. Takayanagi recognised that when one phase is dispersed in another phase there are two limiting possibilities for the stress transfer and Fig. 8 shows the simplified structure of the Takayanagi mechanical coupling model [23], wherein Fig. 8b shows the series–parallel model and Fig. 8c the parallel–series model. For simplicity in Fig. 8b and c we have redefined the structural parameters where u is given by:

$$u = \frac{L_{002}}{L} \tag{6}$$

and

$$w = \frac{b_a}{L_{020} + b_a} \tag{7}$$

It can be shown that for the series–parallel and parallel–series models the modulus is given by [18,22–24]:

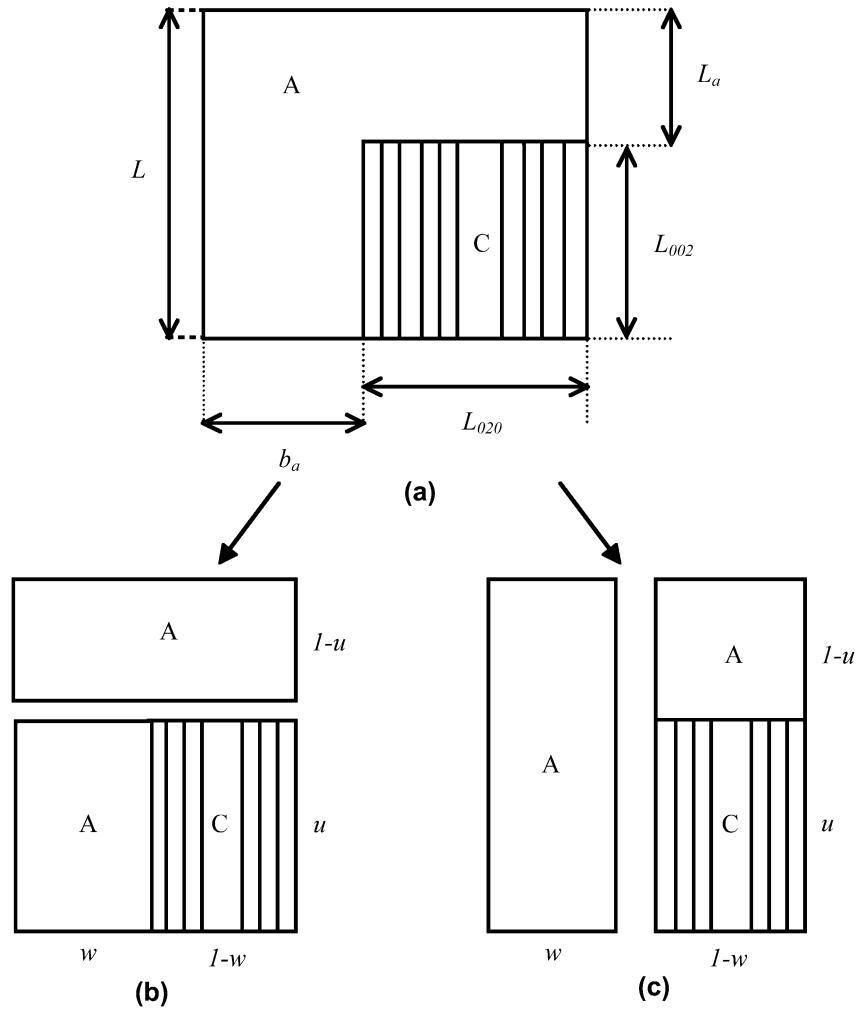

Fig. 8. (a) Takayanagi model; (b) series–parallel model; (c) parallel–series model. L is the long period, L_{020} and L_{002} are the crystallite dimensions in the direction parallel to the normal of the (020) and (002) crystallographic planes of the unit cell, respectively, L_a is the layer of amorphous material connected in series with the crystals and b_a represents the thickness of the amorphous layer connected in parallel with the crystal. A and C denote amorphous and crystalline regions, respectively.

$$\frac{1}{E} = \frac{1-u}{E_A} + \frac{u}{wE_A + E_C(1-w)} \tag{8}$$

and

$$E = wE_A + \frac{E_C(1-w)}{u + (1-u)\dfrac{E_C}{E_A}} \tag{9}$$

where E_A is the modulus of the amorphous material and E_C is the extensional modulus of the crystallite.

For PGA we have obtained the theoretical crystal modulus from the Accelrys software ($E_C = 294$ GPa) and parameters u and w can be easily calculated from the data in Table 3. Hence, in order to predict the modulus of the fibres the only unknown in Eqs. (8) and (9) is the tensile modulus of the amorphous region (E_A).

Fig. 9 shows the experimental tensile modulus of amorphous and highly oriented PGA, together with the predictions using Eqs. (8) and (9) for the series–parallel and parallel–series models, respectively. As can be seen, the series–parallel model is not an adequate representation of the mechanical behaviour of PGA. In contrast, with the parallel–series model, together with the structural data in Table 3, the experimental

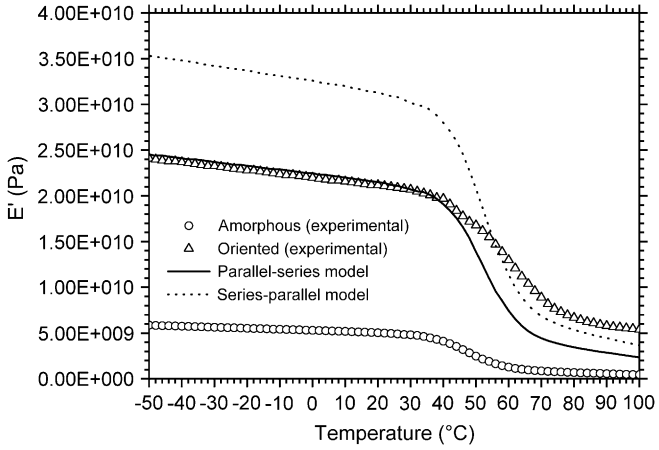

Fig. 9. Experimental and predicted storage moduli (E') of highly oriented PGA fibres using the Takayanagi model, with $E_C = 294$ GPa and the experimental amorphous modulus of PGA, E_A.

values of E_A and the theoretical crystal modulus E_C, we obtain a very good prediction of the extensional modulus of highly oriented PGA below the glass transition temperature (T_g). However, above T_g the prediction is poor with both models and a possible explanation is as follows. It is considered that E_A is the same as in the amorphous isotropic PGA, but it is expected that the amorphous regions connected in parallel with the crystalline blocks contain some ''oriented amorphous material'' whose stiffness and T_g are expected to be slightly higher than that of the isotropic material. Proton NMR studies on highly oriented PGA fibres indicate that indeed the fibres contain three phases with different relaxation times which have been associated with a crystalline phase, an oriented amorphous phase and a completely mobile amorphous phase [18]. Also, the crystal modulus is considered independent of temperature and although small variations are expected, this may cause the model to fail above T_g. Lacks and Rutledge [15] showed that for polyethylene the crystal modulus decreases only about 10% from 0 K to room temperature. We conclude that oriented amorphous material is primarily responsible for the underestimation of the elastic modulus of PGA above the glass transition temperature and that 294 GPa is a reasonable estimate for the crystal modulus of PGA.

As will be discussed below, an important consideration is the relationship between the macroscopic stress (σ_T) and the average crystal strain (ε_C) given by:

$$\sigma_T = E_C^{app}\varepsilon_C \tag{10}$$

where E_C^{app} is the apparent crystal modulus.

It can be shown that for the parallel–series model E_C^{app} is given, respectively, by [18,24,25]:

$$E_C^{app} = wE_A\left(u + (1-u)E_C/E_A\right) + (1-w)E_C \tag{11}$$

The fact that $w > 0$ implies that only an apparent crystal modulus can be measured since the true stress applied in the crystalline region is larger than the macroscopic stress because the latter is based upon the cross-sectional area of the sample, whereas the true stress applied in the crystalline regions is based upon the section $(1-w)$ (see Fig. 8). Nevertheless, a careful examination of Eq. (11) suggests that $E_C^{app} \to E_C$ if the thickness of the amorphous layer in parallel with the crystals is reduced, i.e., $w \to 0$. A second possibility is that if $E_A \to E_C$ then $E_C^{app} \to E_C$, which is less plausible.

For the X-ray crystal strain measurements it can be shown that E_C^{app} is given by:

$$E_C^{app} = -\frac{\sigma_T}{\cot\theta\Delta\theta} \tag{12}$$

where $-\cot\theta\Delta\theta$ is the crystal strain [20] of the (002) reflection of PGA induced by the macroscopic stress σ_T.

Table 4 shows two important calculations using the parallel–series model. From Eq. (9) and the measured values of E_A and E we can extract E_C (calculated) shown in the fourth column in Table 4. The second calculation shown in the last column in this table (E_C^{app} calculated) is obtained with

Table 4
Parallel–series model

Temp. (°C)	E_A (GPa) measured (DMTA)	E (GPa) measured (DMTA)	E_C (GPa) calculated	E_C^{app} (GPa) measured (X-rays)	E_C^{app} (GPa) calculated
−50	5.9	24.1	264	113	170
20	5.1	21.2	289	77	185

Calculated true and apparent crystal modulus with $w = 0.42$ and $u = 0.86$.

Eq. (11), the measured value of E_A and the calculated value of E_C. As can be seen, the calculated values of E_C at −50 and 20 °C are very close to the crystal modulus obtained from the Materials Studio Software (294 GPa). However, the calculated apparent modulus is considerably larger than the value of the apparent modulus measured by X-ray diffraction (see Eq. (12)). For misaligned highly anisotropic fibres the tensile modulus is given by [16]:

$$\frac{1}{E} = \frac{1}{E_C} + \frac{\overline{\sin^2\rho}}{G} \tag{13}$$

We have shown that for highly oriented PGA fibres $\overline{\sin^2\rho} = 0.006$, G is about 6 GPa (see Table 2) and E is 24 GPa (see Table 4), obtaining a value of about $E_C = 230$ GPa and therefore the small misalignment cannot explain the low measured values of E_C^{app} shown in Table 4. It is difficult to explain these quantitative discrepancies without suspecting that the homogeneous stress approximation during deformation is not a valid assumption. However, we have provided enough evidence to conclude that the crystal modulus of PGA is about 294 GPa and that the amorphous regions play a very important role in the overall mechanical behaviour of highly oriented PGA fibres.

4. Conclusions

Theoretical modelling of the elastic behaviour of poly(glycolic acid) (PGA) crystals indicates that the crystal modulus along the chain direction is 294 GPa. It was found that the crystals show a very pronounced mechanical anisotropy due to the planar zigzag conformation of the chains, causing the extensional modulus along the chain axis to be considerably larger than in the other two principal axes of the unit cell.

The structure of highly drawn PGA fibres has been studied by X-ray scattering and calorimetric methods. The fibres possess cylindrical symmetry about the fibre axis and the amorphous and crystalline regions alternate along the fibre axis, with a layer of amorphous material connected in parallel. The mechanical behaviour of PGA fibres was analysed on the basis of this two-phase model and the mechanical properties of the amorphous and crystalline phases, producing a very good correlation between the experimental modulus and the theoretical predictions at temperatures below the glass transition temperature (T_g), consistent with the theoretical value of 294 GPa for the elastic chain modulus. At temperatures above T_g the quantitative discrepancies were explained on the basis of an amorphous partially oriented phase whose stiffness and T_g could be slightly higher than those of the amorphous

isotropic material used to predict the modulus of the fibres in the temperature range −50 to 100 °C.

Acknowledgements

We would like to thank Prof. G.R. Davies and Dr. P.J. Hine for the useful discussions during the preparation of this paper. We would also like to thank Anthony Gleeson for station support at the CLRC Daresbury Laboratories. Dr. Montes de Oca would like to thank Consejo Nacional de Ciencia y Tecnología (CONACyT), México and Smith & Nephew, England for their financial support.

References

[1] Vert M, Li SM, Spenlehauer G, Guerin P. J Mater Sci Mater Med 1992;3:432–46.
[2] Athanasiou KA, Agrawal CM, Barber FA, Burkhart SS. Arthroscopy 1998;14:726–37.
[3] Middleton JC, Tipton AJ. Biomaterials 2000;21:2335–56.
[4] Chatani Y, Suehiro K, Okita Y, Tadokoro H, Chujo K. Makromol Chem 1968;113:215–29.
[5] Montes de Oca H, Ward IM, Klein PG, Ries ME, Rose J, Farrar DF. Polymer 2004;45:7261–72.
[6] Dorset DL. Proc Natl Acad Sci USA 1991;88:5499–502.
[7] Chu CC. J Appl Polym Sci 1981;26:1727–34.
[8] Browning A, Chu CC. J Biomed Mater Res 1986;20:613–32.
[9] Fu BX, Hsiao BS, Chen G, Zhou J, Koyfman I, Jamiolkowsky DD, et al. Polymer 2002;43:5527–34.
[10] Fu BX, Hsiao BS, Chen G, Zhou J, Lin S, Yuan J, et al. Chin J Polym Sci 2003;21:159–67.
[11] Zong X, Ran S, Fang D, Hsiao BS, Chu B. Polymer 2003;44:4959–5967.
[12] von Fraunhofer JA, Sichina WJ. Biomaterials 1992;13:715–20.
[13] Suzuki A, Sato Y, Kunugi T. J Polym Sci B 1998;36:473–81.
[14] Tashiro K, Kobayashi J, Tadokoro H. Macromolecules 1978;11:914.
[15] Lacks DJ, Rutledge GC. J Phys Chem 1994;98:1222–31.
[16] Ward IM. Mechanical properties of solid polymers. 2nd ed. Great Britain: John Wiley & Sons; 1983.
[17] Ward IM. Proc Phys Soc 1962;80:1176–88.
[18] Montes de Oca H. PhD thesis. Production and properties of oriented bioresorbable poly(glycolic acid) fibres. University of Leeds; 2005.
[19] Alexander LE. X-ray diffraction methods in polymer science. USA: John Wiley & Sons; 1969.
[20] Klug HP, Alexander LE. X-ray diffraction procedures for polycrystalline and amorphous materials. 2nd ed. USA: John Wiley & Sons; 1974.
[21] Cohn D, Younes H, Marom G. Polymer 1987;28:2018–22.
[22] Prevorsek DC. Journal of Polymer Science C 1971;32:343–75.
[23] Takayanagi M, Imada K, Kajiyama T. J Polym Sci C 1966;15:263.
[24] Thistlethwaite T, Jakeways R, Ward IM. Polymer 1988;29:61–9.
[25] Thistlethwaite T. PhD thesis. Crystal deformation and structure of oriented poly(ethylene terephthalate) poly(pentamethylene terephthalate) and polyethylene. University of Leeds; 1985.